

**Virtual Hybrid Edge Detection:  
Propagation and recovery of singularities in  
Calderón's inverse conductivity problem**

**Allan Greenleaf**

**University of Rochester, USA**

**with M. Lassas, M. Santacesaria, S. Siltanen and G. Uhlmann**

**LMS–EPSRC Durham Symposium**

**Mathematical and Computational Aspects of Maxwell's Equations**

**July 18, 2016**

---

Partially supported by DMS-1362271 and a Simons Foundation Fellowship

# Electrical impedance tomography (EIT)

Problem: EIT is **high contrast**, but **low resolution**:

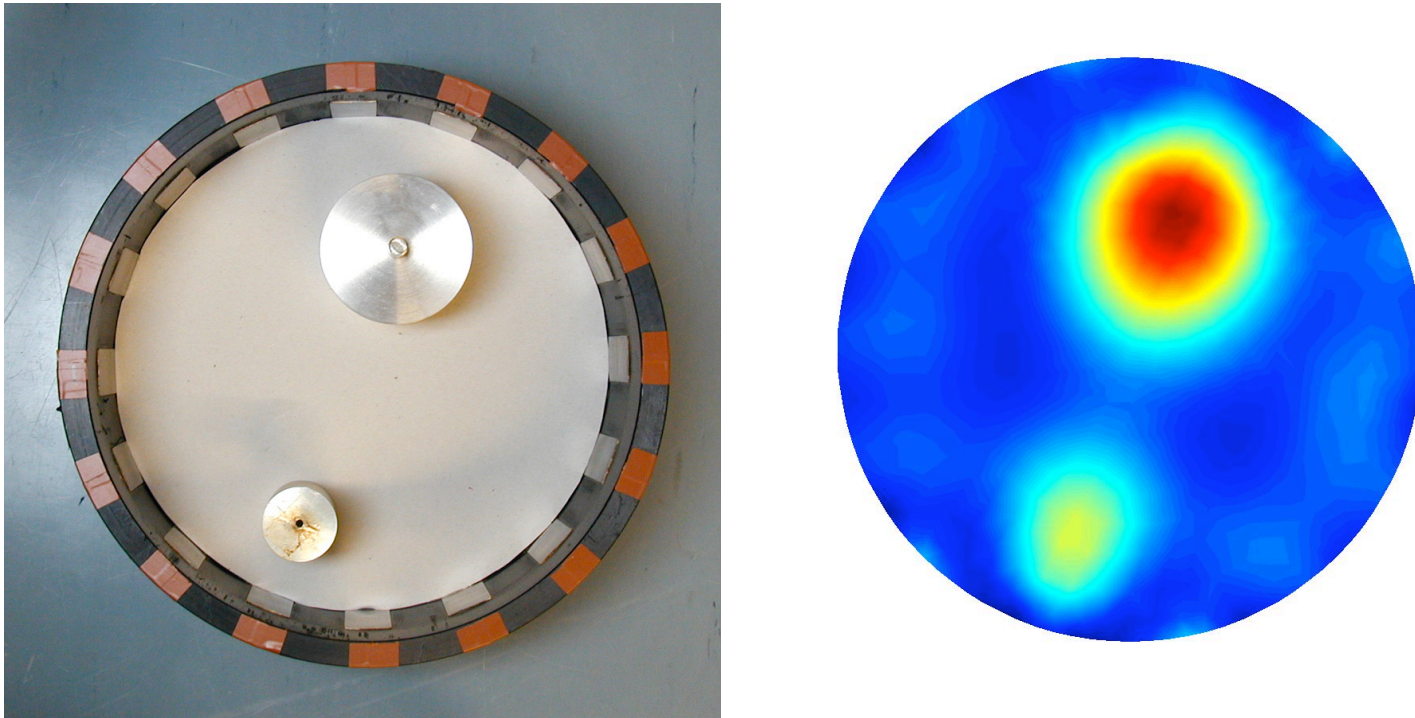


Figure 1: EIT tank and measurements. Source: Kaipio lab, Univ. of Kuopio, Finland

## Hybrid imaging

“Multi-wave” methods often combine illumination and measurement modalities, one having

- **high contrast sensitivity**/low resolution (EIT,..)

and the other exhibiting

- low contrast/**high resolution** (ultrasound...)

## Hybrid imaging

“Multi-wave” methods often combine illumination and measurement modalities, one having

- **high contrast sensitivity**/low resolution (EIT,..)

and the other exhibiting

- low contrast/**high resolution** (ultrasound...)

Use two different types of waves, linked by a **physical coupling**.

## Hybrid imaging

“Multi-wave” methods often combine illumination and measurement modalities, one having

- **high contrast sensitivity** / low resolution (EIT,..)

and the other exhibiting

- low contrast / **high resolution** (ultrasound...)

Use two different types of waves, linked by a **physical coupling**.

Mathematically: couple an **elliptic** PDE with a **hyperbolic / real principal type** PDE

## Current work: virtual 'hybrid' imaging

Use only **one kind of wave**: electrostatic.

Good propagation of singularities is obtained not via coupling with another physics, but by **mathematical analysis**.

## Current work: virtual ‘hybrid’ imaging

Use only **one kind of wave**: electrostatic.

Good propagation of singularities is obtained not via coupling with another physics, but by **mathematical analysis**.

Exploit **complex principal type operator** geometry underlying CGO solutions  $\implies$  Singularities propagate efficiently **along 2D characteristics** to all of  $\partial\Omega$  (in  $\mathbb{R}^2$ ).

## Current work: virtual ‘hybrid’ imaging

Use only **one kind of wave**: electrostatic.

Good propagation of singularities is obtained not via coupling with another physics, but by **mathematical analysis**.

Exploit **complex principal type operator** geometry underlying CGO solutions  $\implies$  Singularities propagate efficiently **along 2D characteristics** to all of  $\partial\Omega$  (in  $\mathbb{R}^2$ ).

Formally: if  $\sigma$  is pws with jumps (**edges**), can stably reconstruct leading singularities.

Can image inclusions within inclusions.

## Astala-Päivärinta CGO solutions in 2D

$\Omega \subset \mathbb{R}^2 = \mathbb{C}$ ,  $(x, y) = x + iy = z$ ,  $(\xi, \eta) = \xi + i\eta = \zeta$

$\sigma \in L^\infty(\Omega)$ ,  $0 < c_1 \leq \sigma(z) \leq c_2 < \infty$ ,

$\sigma \equiv 1$  near  $\partial\Omega$ , extended to  $\mathbb{R}^2$ .

$\implies$  conductivity  $\sigma^{-1}$  is similar

## Astala-Päivärinta CGO solutions in 2D

$\Omega \subset \mathbb{R}^2 = \mathbb{C}$ ,  $(x, y) = x + iy = z$ ,  $(\xi, \eta) = \xi + i\eta = \zeta$   
 $\sigma \in L^\infty(\Omega)$ ,  $0 < c_1 \leq \sigma(z) \leq c_2 < \infty$ ,  
 $\sigma \equiv 1$  near  $\partial\Omega$ , extended to  $\mathbb{R}^2$ .

$\implies$  conductivity  $\sigma^{-1}$  is similar

**Exponentially growing/decaying solutions:**

For  $k \in \mathbb{C}$  a complex frequency,  $\exists u_1, u_2$  s.t.

$$\nabla \cdot \sigma \nabla u_1 = 0, \quad \nabla \cdot \sigma^{-1} \nabla u_2 = 0, \quad \text{on } \mathbb{R}^2,$$

$$u_1, u_2 \sim e^{ikz} \left( 1 + O(1/|z|) \right), \quad |z| \rightarrow \infty.$$

## Beltrami equations

Let  $\mu = \mu_\sigma = \frac{1-\sigma}{1+\sigma}$ , so  $|\mu| \leq 1 - \epsilon$ ,  $\mu_{\sigma-1} = -\mu_\sigma$ .

Look for CGO solns  $f_\mu(z)$  of  $\bar{\partial}_z f_\mu = \mu \overline{\partial_z f_\mu}$ ,  
similarly  $f_{-\mu}$  for  $-\mu$  :

$$f_{\pm\mu}(z, k) = e^{ikz} (1 + \omega^\pm(z, k)), \quad \omega^\pm = O(1/|z|).$$

## Beltrami equations

Let  $\mu = \mu_\sigma = \frac{1-\sigma}{1+\sigma}$ , so  $|\mu| \leq 1 - \epsilon$ ,  $\mu_{\sigma-1} = -\mu_\sigma$ .

Look for CGO solns  $f_\mu(z)$  of  $\bar{\partial}_z f_\mu = \mu \overline{\partial_z f_\mu}$ ,  
similarly  $f_{-\mu}$  for  $-\mu$  :

$$f_{\pm\mu}(z, k) = e^{ikz} (1 + \omega^\pm(z, k)), \quad \omega^\pm = O(1/|z|).$$

$$(u_1, u_2) \leftrightarrow (f_\mu, f_{-\mu})$$

$\omega^\pm$  can be **computed from D2N data** for  $\sigma$ .

**Focus on  $\omega^+ =: \omega$ .**

## Huhtanen and Perämäki solutions (2012)

Let

$$e_k(z) = e^{i(kz + \bar{k}z)} = e^{i2 \operatorname{Re}(kz)},$$

so that  $|e_k(z)| = 1$ ,  $\overline{e_k} = e_{-k}$ .

Define

$$\alpha(z, k) = -i\bar{k}e_{-k}(z)\mu(z), \quad \beta(z, k) = e_{-k}(z)\mu(z)$$

## Huhtanen and Perämäki solutions (2012)

Let

$$e_k(z) = e^{i(kz + \bar{k}z)} = e^{i2 \operatorname{Re}(kz)},$$

so that  $|e_k(z)| = 1$ ,  $\overline{e_k} = e_{-k}$ .

Define

$$\alpha(z, k) = -i\bar{k}e_{-k}(z)\mu(z), \quad \beta(z, k) = e_{-k}(z)\mu(z)$$

Then  $\omega(z, k)$  satisfies a  $\mathbb{R}$ -Beltrami equation:

$$(1) \quad \bar{\partial}\omega - \beta\overline{\partial\omega} - \alpha\bar{\omega} = \alpha.$$

**H.-P.** show that  $\exists! \omega \in W^{1,p}(\mathbb{C})$ ,  $2 < p < p_\epsilon$ .

## Solid Cauchy and Beurling transforms

$$Pf(z) = \frac{1}{\pi} \int_{\mathbb{C}} \frac{f(z')}{z - z'} d^2 z', \quad Sf(z) = -\frac{1}{\pi} \int_{\mathbb{C}} \frac{f(z')}{(z' - z)^2} d^2 z'$$

so that  $\bar{\partial}P = I$ ,  $S = \partial P$  and  $S\bar{\partial} = \partial$  on  $C_0^\infty(\mathbb{C})$ .

## Solid Cauchy and Beurling transforms

$$Pf(z) = \frac{1}{\pi} \int_{\mathbb{C}} \frac{f(z')}{z - z'} d^2 z', \quad Sf(z) = -\frac{1}{\pi} \int_{\mathbb{C}} \frac{f(z')}{(z' - z)^2} d^2 z'$$

so that  $\bar{\partial}P = I$ ,  $S = \partial P$  and  $S\bar{\partial} = \partial$  on  $C_0^\infty(\mathbb{C})$ .

Define  $u = -\partial\bar{\omega} = -\overline{(\partial\omega)} \in L^p$ . Then

$\omega = -P\bar{u}$  and  $\partial\omega = -S\bar{u}$  and (1) becomes

$$(1') \quad (I + A\rho)u = -\bar{\alpha},$$

where  $\rho = \text{complex conjugation}$  and

$$A = -(\bar{\alpha}P + \bar{\beta}S)$$

## Neumann series

**Expand**  $u \sim \sum_{n=0}^{\infty} u_n$ ,  $u_0 = -\bar{\alpha}$ ,  $u_{n+1} = -A\bar{u}_n$

$$\implies \omega = -P\bar{u} \sim \sum_{n=0}^{\infty} \omega_n, \quad \omega_n = -P\bar{u}_n .$$

## Neumann series

**Expand**  $u \sim \sum_{n=0}^{\infty} u_n$ ,  $u_0 = -\bar{\alpha}$ ,  $u_{n+1} = -A\bar{u}_n$

$$\implies \omega = -P\bar{u} \sim \sum_{n=0}^{\infty} \omega_n, \quad \omega_n = -P\bar{u}_n .$$

## Focus on

$$\begin{aligned} u_0 &= -\bar{\alpha}, & \omega_0 &= P\alpha, \\ u_1 &= A\alpha = -(\bar{\alpha}P + \bar{\beta}S)(\alpha), & \omega_1 &= P(\alpha\bar{P}\alpha + \beta\bar{S}\alpha). \end{aligned}$$

## Neumann series

**Expand**  $u \sim \sum_{n=0}^{\infty} u_n$ ,  $u_0 = -\bar{\alpha}$ ,  $u_{n+1} = -A\bar{u}_n$

$$\implies \omega = -P\bar{u} \sim \sum_{n=0}^{\infty} \omega_n, \quad \omega_n = -P\bar{u}_n .$$

## Focus on

$$u_0 = -\bar{\alpha},$$

$$\omega_0 = P\alpha,$$

$$u_1 = A\alpha = -(\bar{\alpha}P + \bar{\beta}S)(\alpha), \quad \omega_1 = P(\alpha\bar{P}\alpha + \beta\bar{S}\alpha).$$

$\omega_0|_{z \in \partial\Omega}$ : **Stably determines singularities of  $\mu$ .**

$\omega_n|_{z \in \partial\Omega}, n \geq 1$ : **Contribute scattering, which explains artifacts in numerics.**

**Note:**  $\omega_n$  is an  $(n + 1)$ -linear operator of  $\mu$ .

We can currently carry this out on level of

- WF set analysis: **all**  $\tilde{\omega}_n$  for **general**  $\sigma \in L^\infty$ .

We can currently carry this out on level of

- WF set analysis: **all**  $\tilde{\omega}_n$  for **general**  $\sigma \in L^\infty$ .
- Operator theory:  $\sigma$  **pws with jumps** across **curved** interfaces  $\implies \tilde{\omega}_1, \tilde{\omega}_2$  are in  $I^{p,l}$  spaces.

We can currently carry this out on level of

- WF set analysis: **all**  $\tilde{\omega}_n$  for **general**  $\sigma \in L^\infty$ .
- Operator theory:  $\sigma$  **pws with jumps** across **curved** interfaces  $\implies \tilde{\omega}_1, \tilde{\omega}_2$  are in  $I^{p,l}$  spaces.
- Higher order terms in Neumann series create a strong artifact at  $t = 0$  and weaker ones via multiple scattering of points in  $WF(\mu)$ .

$$\omega_0(z, k) = \frac{ik}{\pi} \int_{\mathbb{C}} \frac{e^{i2 \operatorname{Re}(kz')} \mu(z')}{z - z'} d^2 z'$$

$$\omega_0(z, k) = \frac{ik}{\pi} \int_{\mathbb{C}} \frac{e^{i2 \operatorname{Re}(kz')} \mu(z')}{z - z'} d^2 z'$$

1. Polar coordinates in  $k$ : write  $k = \tau e^{i\varphi}$

$$\omega_0(z, k) = \frac{ik}{\pi} \int_{\mathbb{C}} \frac{e^{i2 \operatorname{Re}(kz')} \mu(z')}{z - z'} d^2 z'$$

1. Polar coordinates in  $k$ : write  $k = \tau e^{i\varphi}$
2. Partial Fourier transform  $\tau \rightarrow t$ :

$$\begin{aligned} \tilde{\omega}_0(z, t, e^{i\varphi}) &:= \int_{\mathbb{R}} e^{-it\tau} \omega_0(z, \tau e^{i\varphi}) d\tau \\ &= \frac{e^{i\varphi}}{\pi} \int_{\mathbb{R}} \int_{\mathbb{C}} (i\tau) \frac{e^{-i\tau(t-2 \operatorname{Re}(e^{i\varphi} z'))}}{z - z'} \mu(z') d^2 z' d\tau \\ &= -2e^{i\varphi} \int_{\mathbb{C}} \frac{\delta'(t - 2 \operatorname{Re}(e^{i\varphi} z'))}{z - z'} \mu(z') d^2 z' \end{aligned}$$

**Recall:**  $\sigma \in L^\infty$ ,  $\sigma \equiv 1$  near  $\partial\Omega$ ,  $\mu \equiv 0$  near  $\partial\Omega$ .

**Assume**  $\text{supp}(\mu) \subset \Omega_0 \subset\subset \Omega$ .

**Define**  $T_0 : \mathcal{E}'(\Omega_0) \rightarrow \mathcal{D}'(\mathbb{C} \times \mathbb{R} \times \mathbb{S}^1)$ ,

$$\mu(z') \longrightarrow (T_0\mu)(z, t, e^{i\varphi}) := \tilde{\omega}_0(z, t, e^{i\varphi}).$$

**Recall:**  $\sigma \in L^\infty$ ,  $\sigma \equiv 1$  near  $\partial\Omega$ ,  $\mu \equiv 0$  near  $\partial\Omega$ .

Assume  $\text{supp}(\mu) \subset \Omega_0 \subset\subset \Omega$ .

Define  $T_0 : \mathcal{E}'(\Omega_0) \rightarrow \mathcal{D}'(\mathbb{C} \times \mathbb{R} \times \mathbb{S}^1)$ ,

$$\mu(z') \longrightarrow (T_0\mu)(z, t, e^{i\varphi}) := \tilde{\omega}_0(z, t, e^{i\varphi}).$$

Schwartz kernel of  $T_0$ :

$$K_0(z, t, e^{i\varphi}, z') = \left( \frac{-2e^{i\varphi}}{z - z'} \right) \delta'(t - 2 \operatorname{Re}(e^{i\varphi} z')).$$

First factor is smooth for  $z \notin \Omega_0$ ,  $z' \in \Omega_0 \implies$

$T_0$  is a **generalized Radon transform** and thus a **Fourier integral operator (FIO)**.

**Define**  $T_0^{z_0} : \mathcal{E}'(\Omega_0) \rightarrow \mathcal{D}'(\mathbb{R} \times \mathbb{S}^1)$  **by**

$$\mu(z') \longrightarrow (T_0^{z_0} \mu)(t, e^{i\varphi}) := \tilde{\omega}_0(z_0, t, e^{i\varphi}).$$

Define  $T_0^{z_0} : \mathcal{E}'(\Omega_0) \rightarrow \mathcal{D}'(\mathbb{R} \times \mathbb{S}^1)$  by

$$\mu(z') \longrightarrow (T_0^{z_0} \mu)(t, e^{i\varphi}) := \tilde{\omega}_0(z_0, t, e^{i\varphi}),$$

- $T_0^{z_0}$  is a **weighted and differentiated** version of the Radon transform on  $\mathbb{C} \simeq \mathbb{R}^2$ .

- $T_0^{z_0}$  is an FIO of order  $\frac{1}{2}$ ,  $T_0^{z_0} \in I^{\frac{1}{2}}(C)$ , with same canonical relation as std. Radon transf.

$$C = N^* \{t = 2 \operatorname{Re}(e^{i\varphi} z')\}' \subset T^*(\mathbb{R} \times \mathbb{S}^1) \times T^*\Omega_0.$$

- $C$  is a **canonical graph**.

- $C$  is **independent of  $z_0$** , but symbol

$$\sigma_{prin}(T_0^{z_0}) = \frac{(-ie^{i\varphi}) \operatorname{sgn}(\tau) |\tau|^{\frac{1}{2}}}{z_0 - z'},$$

is not.

- The factor  $(z_0 - z')^{-1}$  is smooth and  $\neq 0$ , but causes

(i) A **fall-off in detectability** of jumps, at rate  $\sim d(z', z_0)^{-1}$ .

(ii) **Artifacts**, esp. when  $\mu$  has singularities at  $z'$  close to  $z_0$ , due to the large **magnitude** and **phase gradient** of  $(z_0 - z')^{-1}$ .

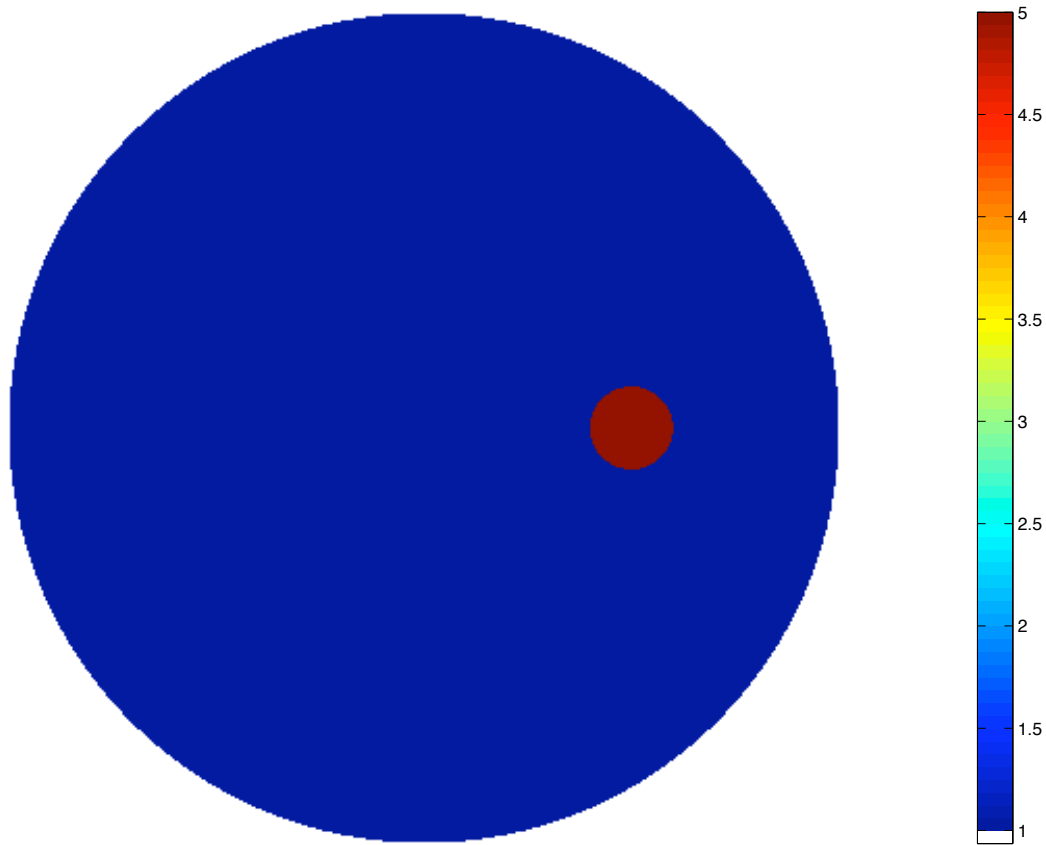


Figure 2: Conductivity phantom: a small circular inclusion.

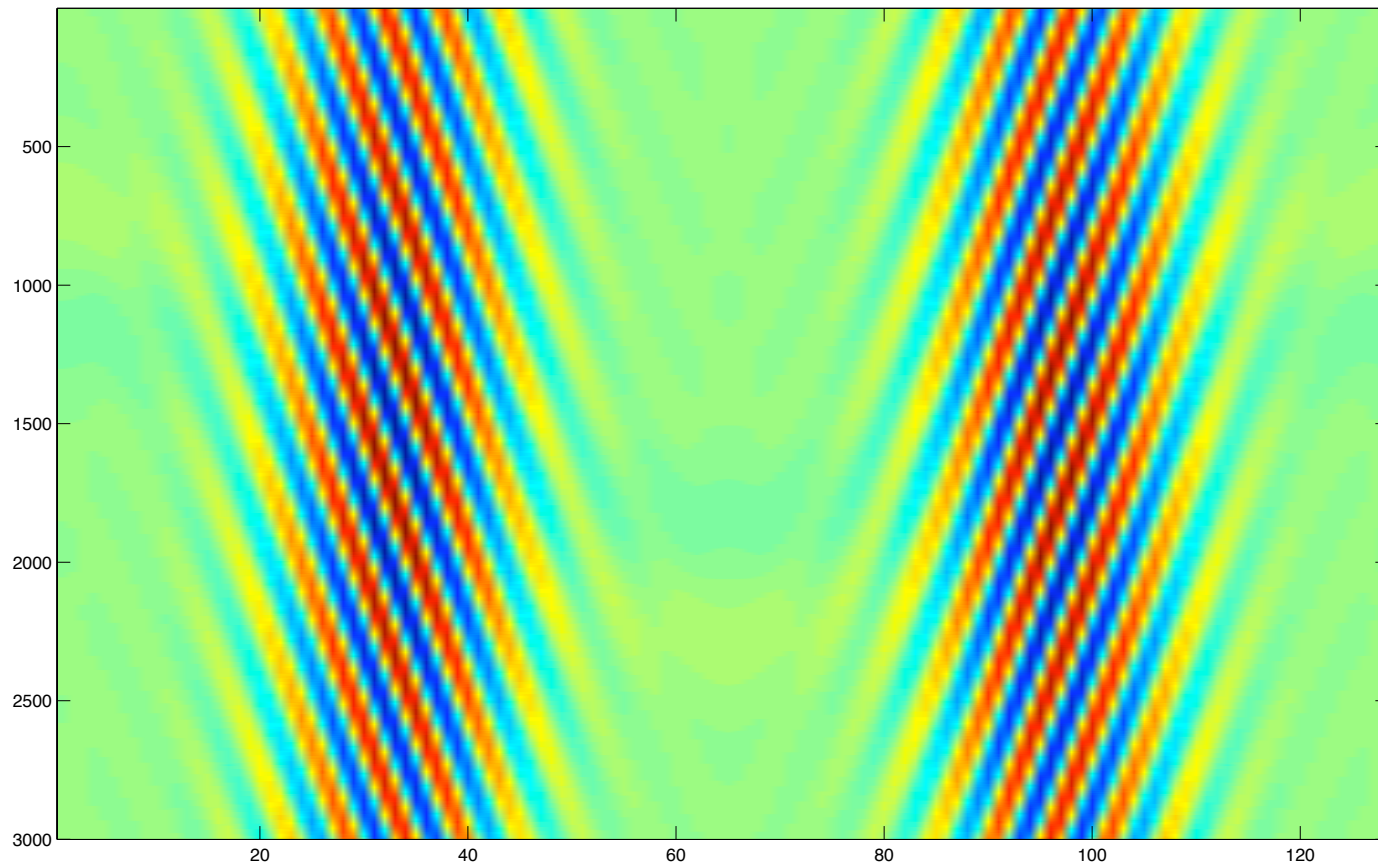


Figure 3:  $Re \tilde{\omega}(z_0, t, e^{i\varphi})$  (axes:  $\varphi = \text{horiz.}$ ,  $t = \text{vert.}$ )

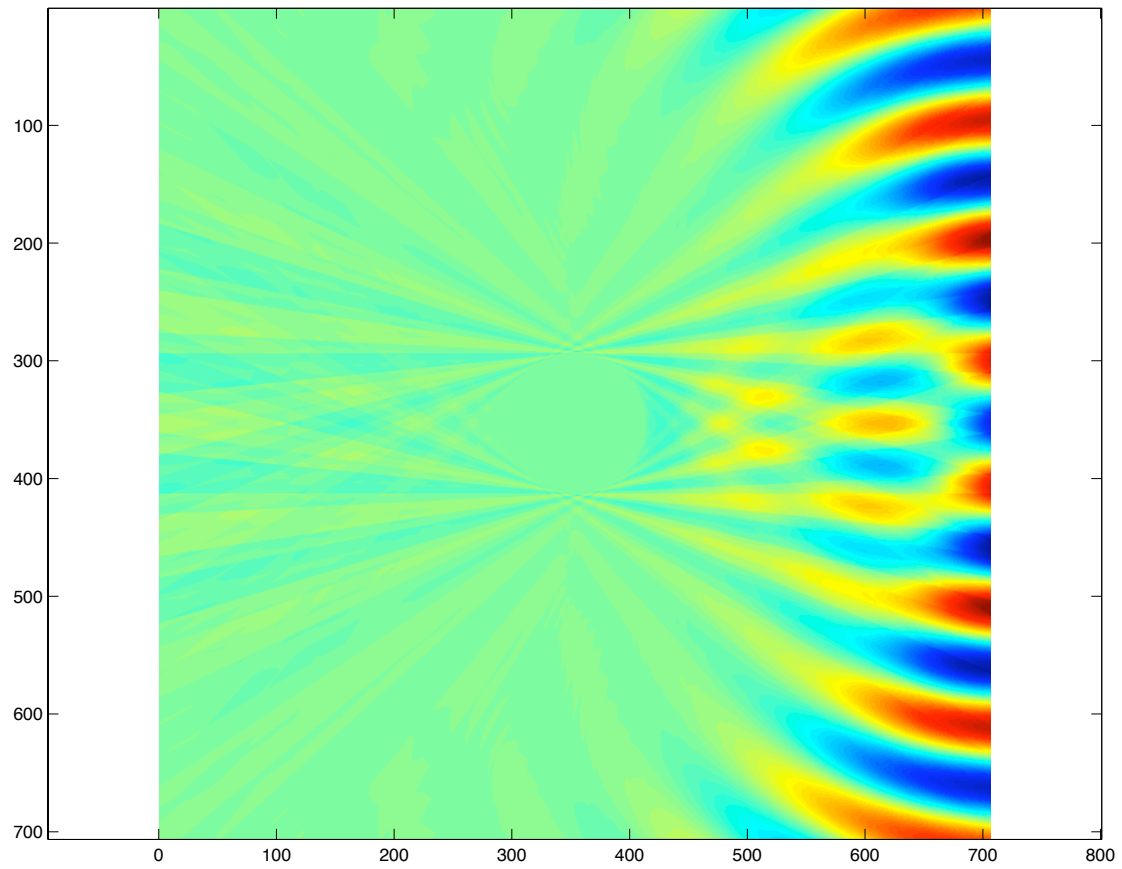


Figure 4: Backprojected reconstruction from  $\omega(z_0, \cdot, \cdot)$ .

## Weighted ‘averages’ in $z_0$

Let  $a(z_0)$  be a  $\mathbb{C}$ -valued weight on  $\partial\Omega$ . Form

$$(3) \quad \tilde{\omega}_0^a(t, \varphi) := \frac{1}{2\pi i} \int_{\partial\Omega} \tilde{\omega}_0(z_0, t, \varphi) a(z_0) dz_0,$$

Let  $T_0^a$  be the operator  $\mu \rightarrow \tilde{\omega}_0^a$ .

## Weighted ‘averages’ in $z_0$

Let  $a(z_0)$  be a  $\mathbb{C}$ -valued weight on  $\partial\Omega$ . Form

$$(2) \quad \tilde{\omega}_0^a(t, \varphi) := \frac{1}{2\pi i} \int_{\partial\Omega} \tilde{\omega}_0(z_0, t, \varphi) a(z_0) dz_0,$$

Let  $T_0^a$  be the operator  $\mu \rightarrow \tilde{\omega}_0^a$ .

Then  $T_0^a \in I^{\frac{1}{2}}(C)$  and  $(T_0^a)^* T_0^a \in \Psi^1(\Omega_0)$ , with

$$\sigma_{prin}((T_0^a)^* T_0^a)(z', \zeta') = 2\pi^2 |\alpha(z')|^2 |\zeta'|, \quad z' \in \Omega_0,$$

where

$$\alpha(z') = \frac{1}{2\pi i} \int_{\partial\Omega} \frac{a(z_0) dz_0}{z_0 - z'}, \quad z' \in \Omega$$

is the **Cauchy (line) integral** of  $a(\cdot)$

**Pick  $a \equiv 1/\sqrt{2}$  on  $\partial\Omega$  in (2). ( $\int_{\partial\Omega} a dz_0 = 0!$ )**

**Then  $\alpha(z') \equiv 1/\sqrt{2}$  on  $\Omega_0$  and**

$$(T_0^a)^* T_0^a = (-\Delta)^{\frac{1}{2}} \text{ mod } \Psi^0(\Omega_0),$$

Pick  $a \equiv 1/\sqrt{2}$  on  $\partial\Omega$  in (3). ( $\int_{\partial\Omega} a dz_0 = 0!$ )

Then  $\alpha(z') \equiv 1/\sqrt{2}$  on  $\Omega_0$  and

$$(T_0^a)^* T_0^a = (-\Delta)^{\frac{1}{2}} \text{ mod } \Psi^0(\Omega_0),$$

Gives local-tomography type imaging of  $\mu$ , good for **detection of singularities** of  $\sigma$  from the singularities of  $\tilde{\omega}$  (which correspond to high frequency behavior of  $\omega$ ).

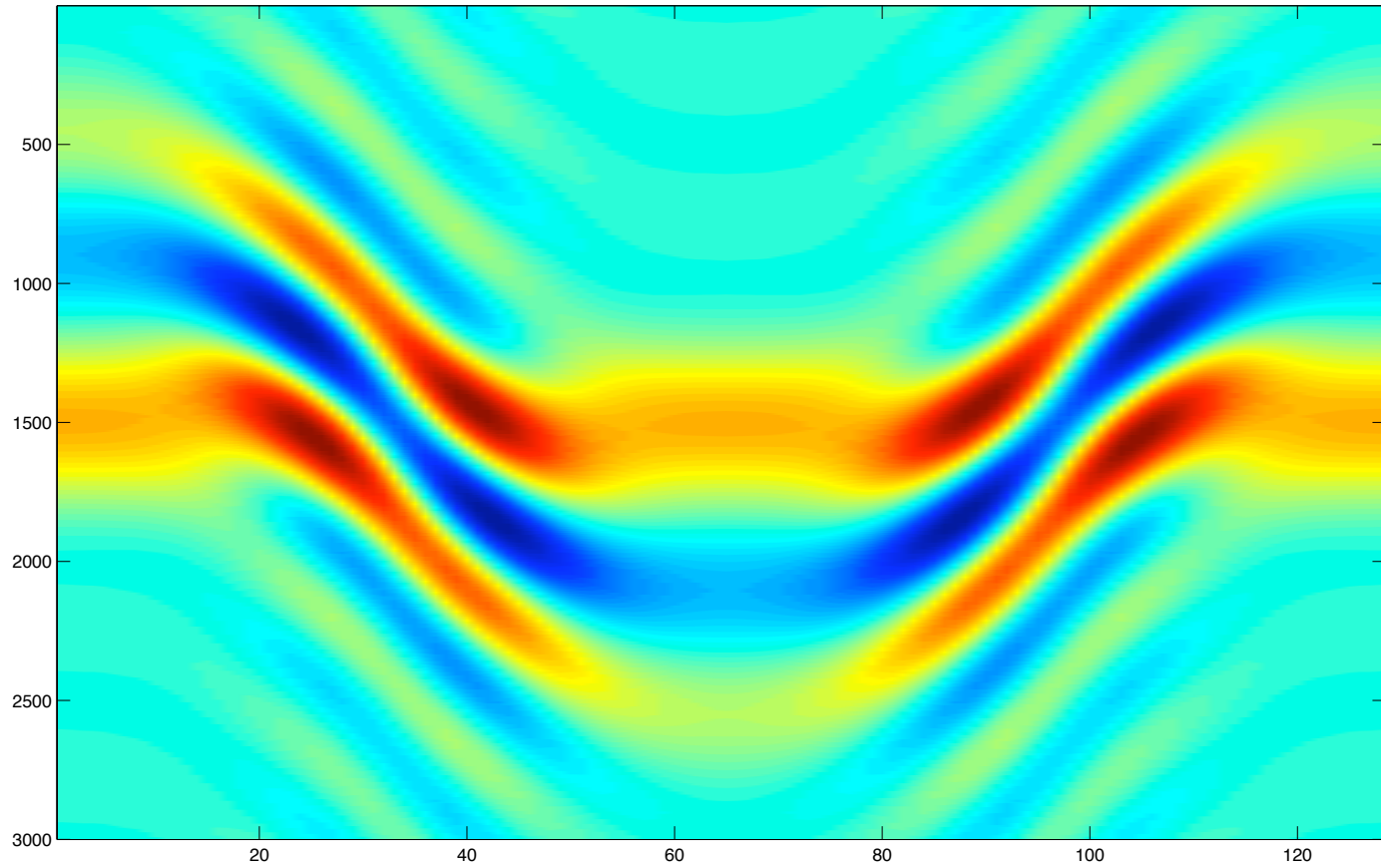


Figure 5:  $Re \tilde{\omega}^a(z_0, t, e^{i\varphi})$  for  $a \equiv 1/(2\sqrt{2})$

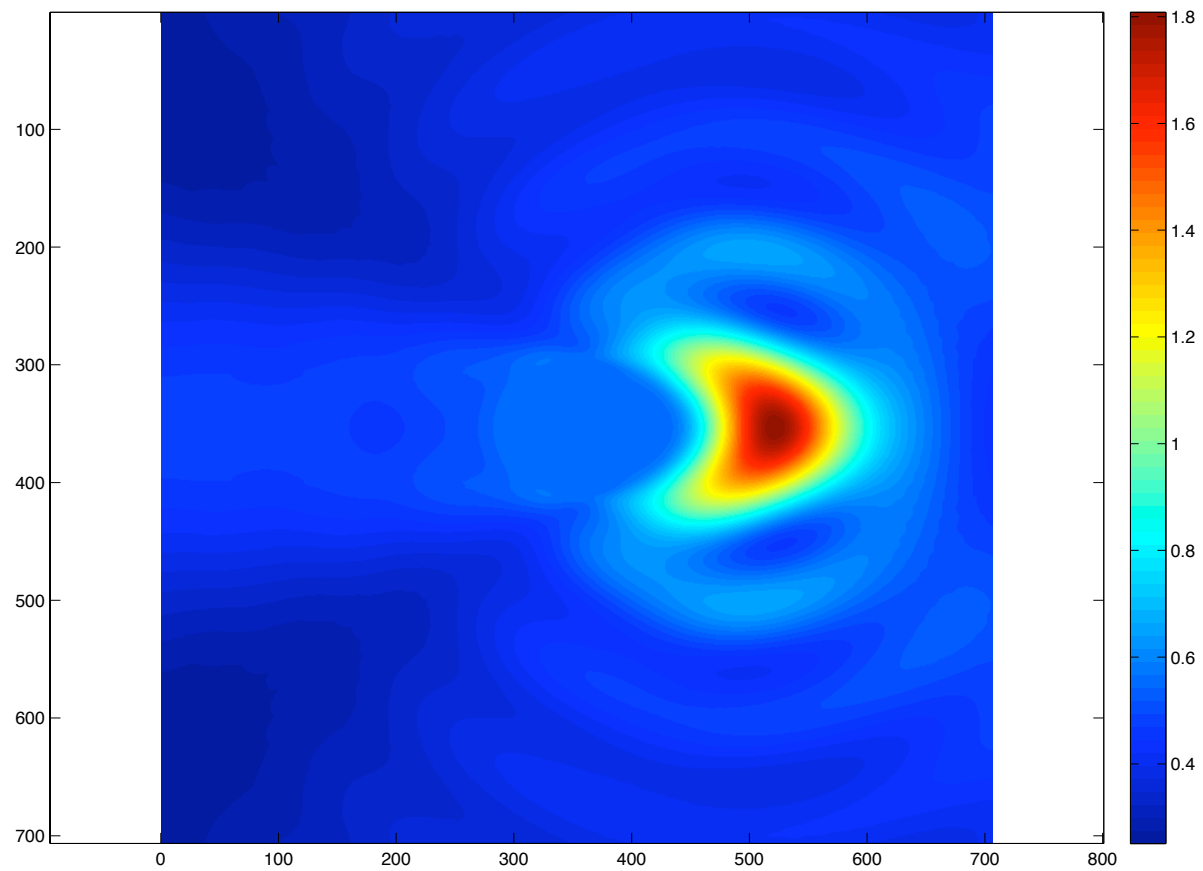


Figure 6: Reconstruction from  $\tilde{\omega}^a(\cdot, \cdot)$  for  $a \equiv 1/\sqrt{2}$ .

So far, microlocal analysis **does not seem to be needed:** can express  $\omega_0^a$  in terms of the Radon transform.

However: the figures above were created after **filtering out certain artifacts.**

So far, microlocal analysis **does not seem to be needed**: can express  $\omega_0^a$  in terms of the Radon transform.

However: the figures above were created after **filtering out certain artifacts**.

Singularities of  $\tilde{\omega}^{z_0}, \tilde{\omega}^a$  occur at

- (i)  $t = 0$  for **any**  $\mu$  with singularities, and
- (ii) at other values of  $t, \varphi$ , **depending on**  $\mu$ .

Explained by **wave-front set analysis** of the higher order terms in the Neumann series, which are **multilinear FIOs**.

$$\begin{aligned}
\tilde{\omega}_1^{z_0}(t, \varphi) &= \int e^{-it\tau} \omega_1(z_0, \tau e^{i\varphi}) d\tau \\
&= \int_{\Omega} \int_{\Omega} K_1^{z_0}(t, e^{i\varphi}; z', z'') \cdot \mu(z') \cdot \mu(z'') d^2 z' d^2 z''
\end{aligned}$$

**Bilinear operator** acting on  $\mu \otimes \mu$ , w/ kernel

$$\begin{aligned}
K_1^{z_0}(t, e^{i\varphi}; z', z'') &= \frac{1}{\pi^2} \left( \frac{e^{2i\varphi} \delta''(t + 2 \operatorname{Re}(e^{i\varphi}(z' - z''))) }{(z' - z_0)(\bar{z}'' - \bar{z}')} \right) \\
&\quad + \frac{e^{i\varphi} \delta'(t + 2 \operatorname{Re}(e^{i\varphi}(z' - z''))) }{(z' - z_0)(\bar{z}'' - \bar{z}')^2}
\end{aligned}$$

- $WF(\tilde{\omega}_n)$  can be described in terms of  $(n + 1)$ -fold scatterings of  $WF(\mu)$ .
- Still to do: estimates to control smoothness of  $\tilde{\omega}_n$  for  $n \geq 3$ .

- $WF(\tilde{\omega}_n)$  can be described in terms of  $(n + 1)$ -fold scatterings of  $WF(\mu)$ .
- Still to do: estimates to control smoothness of  $\tilde{\omega}_n$  for  $n \geq 3$ .
- Can currently do this for  $n = 1, 2$  under prior on  $\sigma$  which includes pws with jumps across curved interfaces.
- Rigorous justification of the Neumann series will require a mixture of multilinear **microlocal** and **harmonic** analysis.

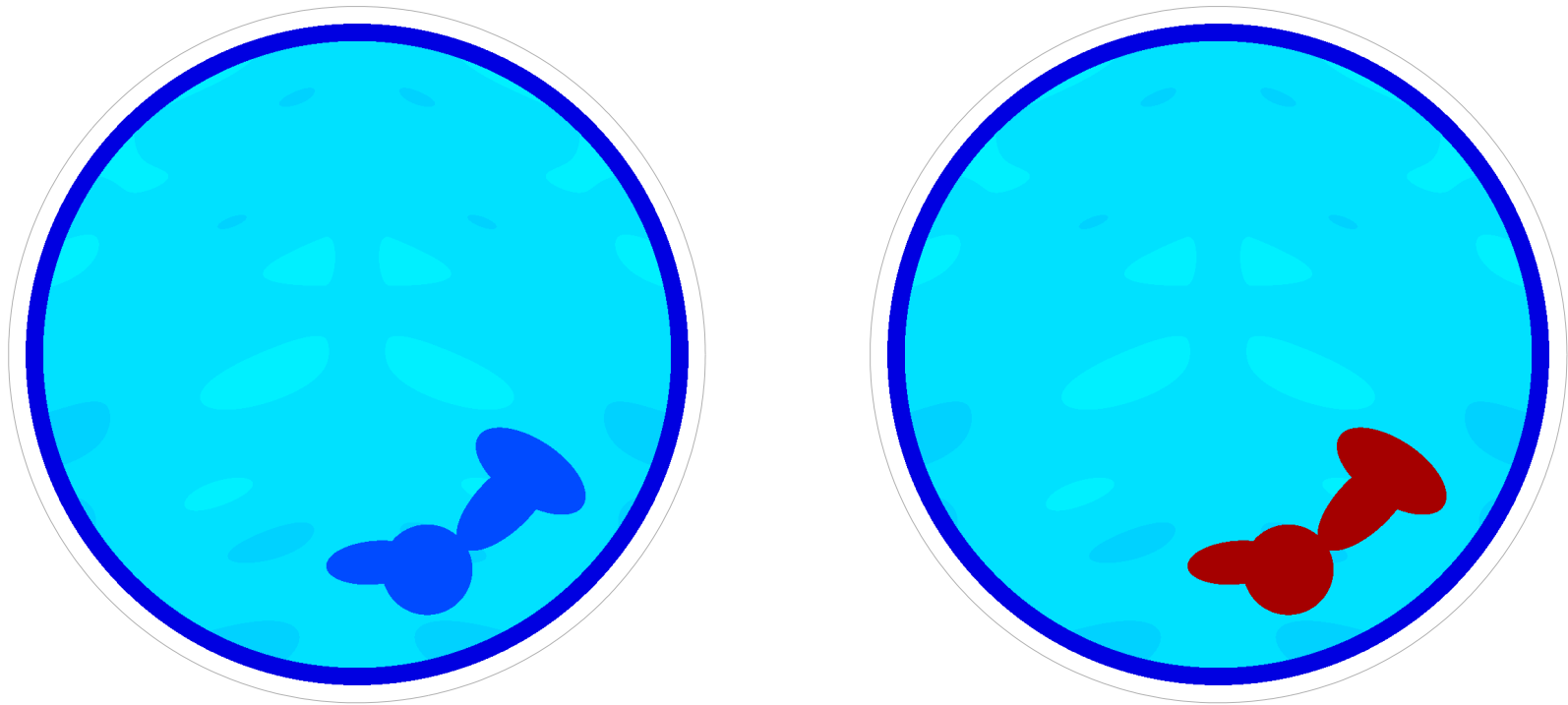


Figure 7: Stroke phantoms within low conductivity skull: Clot (**left**), haemorrhage (**right**).

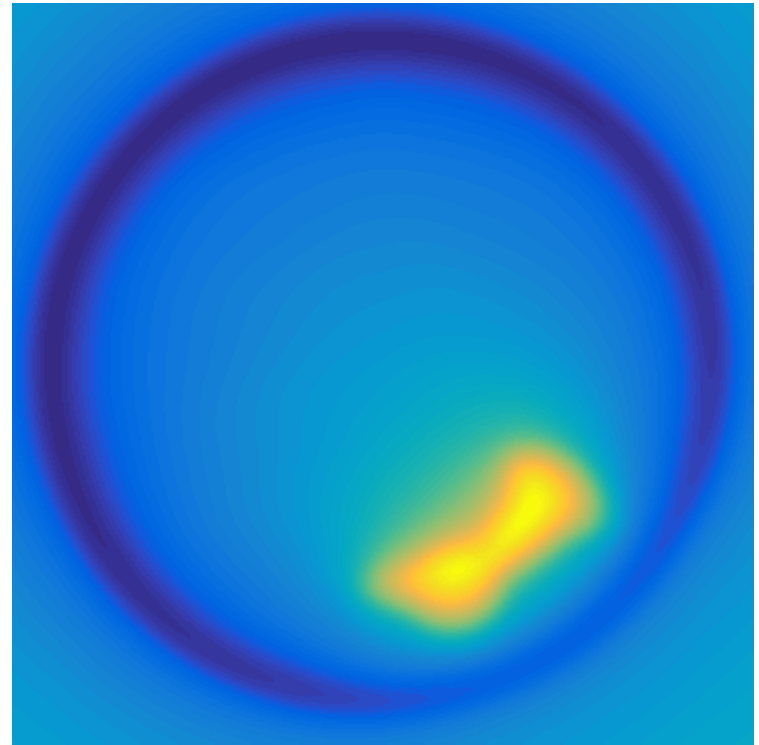
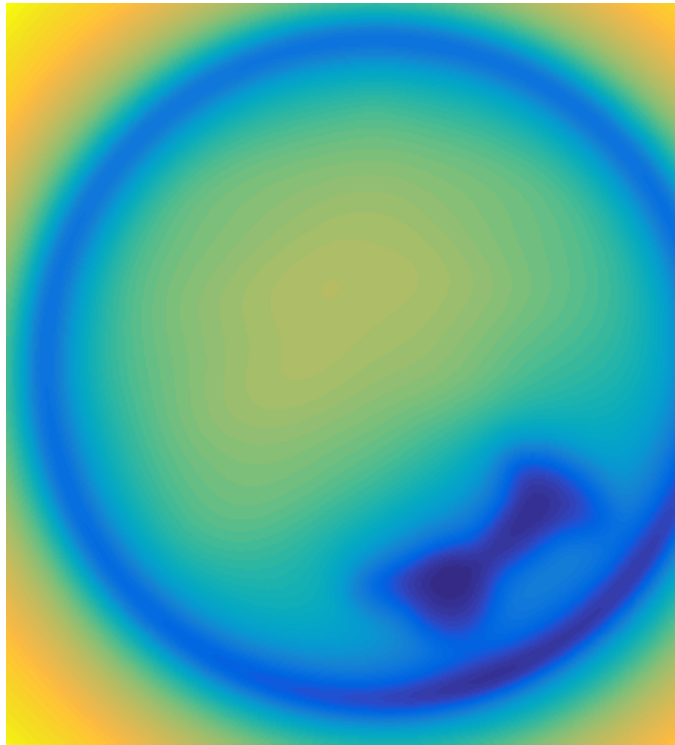


Figure 8: Stroke phantoms reconstructions: Clot (**left**),  
haemorrhage (**right**).